



# PHOTOCATALYTIC DEGRADATION OF AZO DYE CONGO RED USING ZINC SUBSTITUTED NICKEL FERRITE

S. B. Narde<sup>a</sup>, R.B.Lanjewar<sup>b</sup>, S. M. Gadegone<sup>c</sup>, M. R.Lanjewar<sup>d</sup>

<sup>a</sup>D.B.Science College, Gondia-441614, <sup>b</sup>Dharampeth M.P.Deo Memorial Science College, Nagpur, <sup>c</sup>Kamla Nehru Mahavidyalaya, Nagpur, <sup>d</sup>PG Department of Chemistry, RTMNU, Nagpur

## ABSTRACT

**Photo catalytic degradation of azo dye Congo Red in aqueous solution was studied using cubic spinel mixed metal ferrite with compositional formula  $\text{Ni}_{0.4}\text{Zn}_{0.6}\text{Fe}_2\text{O}_4$  synthesized by sol-gel auto combustion method. The synthesis was carried out at pH 7 and the sample was annealed at  $800^\circ\text{C}$ . The ferrite sample was characterized using XRD, FTIR, SEM-EDX and TEM techniques. The photo catalytic efficiency of the synthesized sample against Congo Red dye in aqueous solution was investigated in the presence of short wave UV light for 100ml dye solution for contact time 120 min. The photo degradation experiments were carried out w. r. t. effect of pH, catalyst loading, different dye concentration and the influence of these parameters on photo degradation of dye was studied. The photo degradation efficiency of ferrite was found to be maximum at pH 3 for 0.2g ferrite for 100mL of 10 mg/L dye solution. The pseudo first order kinetics of photo degradation was studied using Langmuir-Hinshelwood model.**

**Keywords: Auto-combustion, Congo Red, Ni-Zn nanoferrites, Photo catalytic degradation**

## Introduction

Water is one of the most important components of the biosphere. Ground water and surface water pollution is a severe problem to the environment due to its high toxicity for the presence of dyes and organic waste. The extent of industrial water pollution and industrialization has a direct impact on living beings [1]. Waste water from various textile industries containing synthetic dyes such as azo dyes is the major water pollutant. Thus, it

becomes necessary to develop new methods to remove colored effluents before discharging them into environment [2, 3]. In recent years, semiconductor-assisted photo-catalysis has come up as a promising tool as a substitute to the traditional wastewater treatment. It has attracted the researchers due to its ability to convert toxic waste into nontoxic products [4]. Further, the process is cost effective, highly efficient, consumes low energy and decreases secondary pollution [5]. The aim of the present study is to investigate photo catalytic efficiency of the novel ferrite material synthesized by sol gel auto combustion method over Congo red dye [6].

## Experimental

### 2.1 Materials

AR Grade Iron nitrate nonahydrate  $\text{Fe}(\text{NO}_3)_3 \cdot 9\text{H}_2\text{O}$ , Nickel nitrate hexahydrate  $\text{Ni}(\text{NO}_3)_2 \cdot 6\text{H}_2\text{O}$ , Zinc nitrate hexahydrate  $\text{Zn}(\text{NO}_3)_2 \cdot 6\text{H}_2\text{O}$ , citric acid and liquor ammo, Congo Red obtained from SD fine-chem limited with high purity of 99.99% and used without further purification.

### 2.2 Method

Nickel zinc ferrite Nanoparticles with compositional formula  $\text{Ni}_{0.6}\text{Zn}_{0.4}\text{Fe}_2\text{O}_4$  were synthesized by sol gel auto-combustion method by dissolving fixed amounts of nitrate precursors and citric acid (molar ratio 1:1) separately in minimum amount of distilled water and mixing together with constant stirring at room temperature. The pH value of the solution was adjusted by adding ammonia solution. The solution was then continuously stirred and slowly heated using a hot plate magnetic stirrer at  $80^\circ\text{C}$  till a very viscous gel formed got ignited and burnt in a self-

propagating combustion manner to obtain loose powder which was then ground in an agate mortar for half an hour, annealed at 800°C in a muffle furnace for 2 hrs.

### 2.3 Characterization Techniques

To determine the structure of prepared sample X-ray diffraction studies was carried out by using Bruker AXS, D8 Advance spectrophotometer with Cu-K $\alpha$  radiation ( $\lambda=1.5418 \text{ \AA}$ ) in a wide range of Bragg's angle (20-80°C) at room temperature. An infrared spectrum of the powder sample was recorded using Fourier Transform Infra-Red Spectrophotometer (FTIR Nicolet, Avatar 370 model) by the KBr pellet method. The microstructure of the powdered sample was investigated using Scanning Electron Microscope (JEOL Model JSM-6390LV). Elemental analysis was carried out by using Energy Dispersive Spectrometer (JEOL Model JED-2300) TEM studies of the ferrite was performed using Transmission Electron Microscope JEOL Model JSM - 6390LV.

### 2.4 Photo catalytic activity

Photo degradation study for Congo red (synonyms-C.I. Direct red28, Cotton red.C.I.22120, molecular weight=696.67 gmol<sup>-1</sup>, C<sub>32</sub>H<sub>22</sub>N<sub>6</sub>Na<sub>2</sub>O<sub>6</sub>S<sub>2</sub>) was performed by batch experiments. Photo degradation experiments were carried out in presence of short wavelength UV light (254 nm). Zinc substituted nickel ferrite with compositional formula Ni<sub>0.6</sub>Zn<sub>0.4</sub>Fe<sub>2</sub>O<sub>4</sub> was used as photo catalyst. The pH of the dye solution was adjusted using 0.1 N HCl and 0.1 N NaOH solutions and recorded on digital pH meter. The dye solution was stirred well as well as aerated and 5 ml samples were withdrawn at regular time interval of 30 min,

centrifuged for 5 min to remove photo catalyst completely and absorbance was measured using Shimadzu UV1800 spectrophotometer. The percentage degradation was calculated by using the formula:

$$\text{Percentage degradation} = \{(A_0 - A_t) \div A_0\} \times 100$$

Where, A<sub>0</sub> is the initial absorbance of the dye solution, A<sub>t</sub> is the absorbance at time interval 't'.

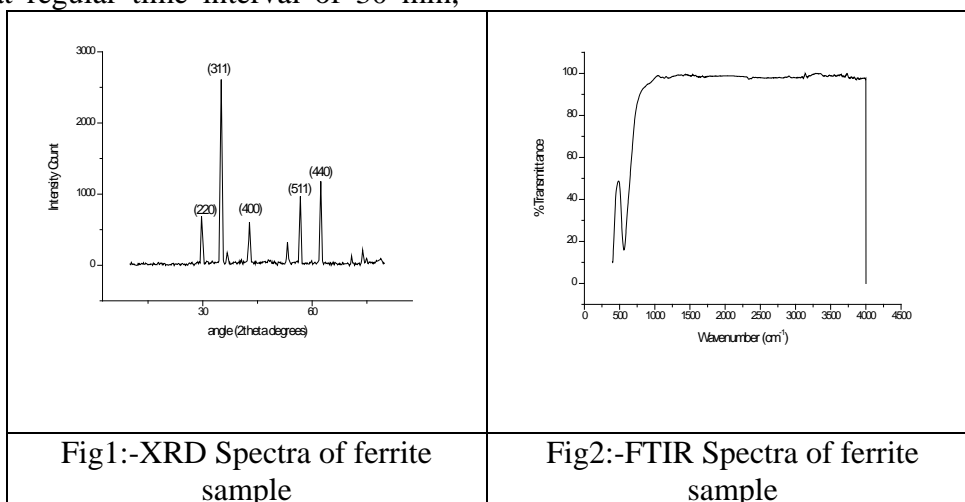
## Result and Discussion

### 3.1 X-Ray Diffraction studies

XRD pattern of the synthesized ferrite is shown in the Fig. 1. It confirms the formation of single phase cubic spinel structures. It shows all the characteristic peaks corresponding to the characteristic planes which appear at their respective 2 $\theta$  values for face centered cubic ferrite nanoparticles matched with JCPDS standard powder diffraction card No. 52-0278 having space group Fd3m (227). Most intense peak (311) at 35.51° was used to calculate crystallite size using Debye Scherer's formula [7]. The average crystallite size and lattice parameter of the ferrite samples was found to be 41.97 nm and 8.332 Å respectively.

### 3.2 Fourier Transform Infrared Spectroscopy

FT-IR spectrum of the ferrite sample is shown in Fig. 2. The intense peak at 566.61 cm<sup>-1</sup> can be attributed to intrinsic Fe-O vibration of tetrahedral Fe<sup>3+</sup> and another peak near 400 cm<sup>-1</sup> to that of octahedral Fe<sup>2+</sup> sites [8] which support the spinel structure of synthesized ferrite samples.



### 3.3 Scanning Electron Microscopy and Elemental Analysis

SEM image and EDX pattern of ferrite sample are shown in Fig.3a-b, respectively. SEM micrograms show formation of largely agglomerated well defined nanoparticles with

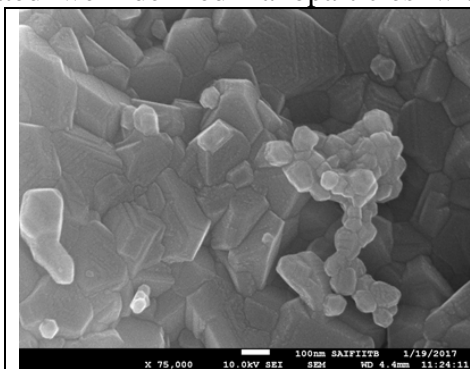


Fig. 3a:- FE-SEM image of ferrite system

irregular morphology. The EDX pattern obtained for ferrite gives the elemental and atomic composition in the sample. The compound shows the presence of Ni, Zn, Fe and O.

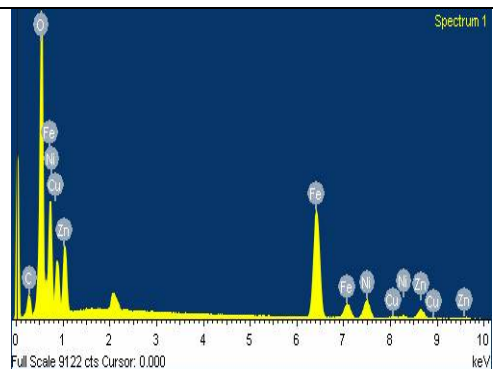


Fig. 3b:- EDX pattern of ferrite system

### 3.4 Transmission Electron Microscopy

Fig. 4a-b show the TEM images of ferrite sample. It is observed that most of the particles are in nano-meter scale and are mostly of elongated spherical shape with a narrow size distribution and agglomeration. The results obtained are in good agreement with the size calculated from peak broadening in X-ray

diffraction pattern. Also, the selected area electron diffraction pattern (SAED) consists of concentric rings with bright spots over the rings indicating polycrystalline nature of the sample. The rings are consistent with the cubic spinel structure with an intense ring pattern from (hkl) plane.

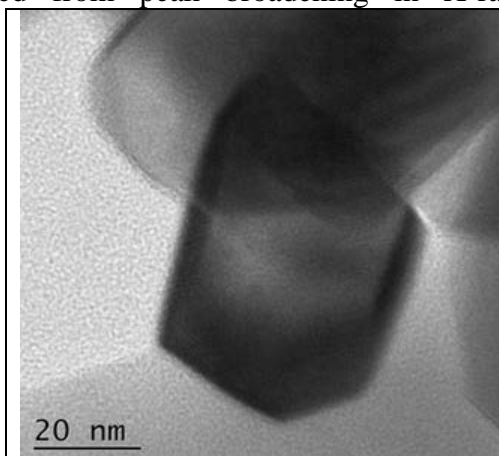


Fig.4a:- TEM image of ferrite system

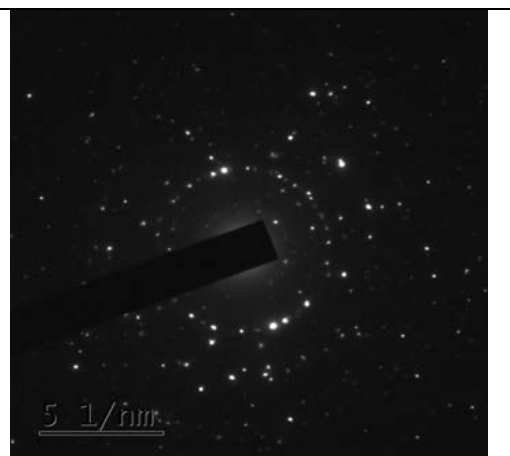


Fig.4b:- SAED pattern of ferrite system

### 3.5 Photo degradation of Congo red

The photocatalytic degradation of Congo red assisted by synthesized ferrite in aqueous solution was studied in presence of short wave UV light for 100 ml dye solution and the influence of following parameters on degradation was studied.

#### 3.5.1 Effect of pH

The role of pH on degradation of organic pollutants catalyzed by heterogeneous photo catalyst is important because the particle size,

surface charge and band edge positions of the semiconductor oxide are strongly influenced by the effect of pH [9]. It also has influence on the dye molecule charge. To determine the optimum pH conditions for the photo degradation of Congo red, the effect of pH was studied using ferrite  $\text{Ni}_{0.4}\text{Zn}_{0.6}\text{Fe}_2\text{O}_4$  over the pH range of 3 - 10 with a stirring time of 30 min for  $10\text{mgL}^{-1}$  dye solution and  $0.1\text{g } 100\text{mL}^{-1}$  catalyst dosage for all experiments. The results obtained are presented in Fig. 5a-b. The

maximum photocatalytic activity was observed at pH 3 for the photo catalyst and decreases gradually up to pH 10. It may be due to the variation of surface charge of ferrite nanoparticle as a function of pH of the solution. This result is also supported by  $pH_{pzc}$  (point of zero charge). The observed  $pH_{pzc}$  is in the range of pH 2-3 for all these ferrites, so the charge on the particles near this pH is zero [10]. The surface charge is positive at pH values lower than  $pH_{pzc}$ , neutral at  $pH_{pzc}$  and negative at pH values higher than it. As at  $pH > pH_{pzc}$  of the adsorbent, the solid surface is negatively charged, it repels  $R-SO_3^-$  ions of CR. Therefore, degradation efficiency decreases in alkaline samples [11]. pH = 2 is avoided here because CR dye sediments rapidly at pH = 2 with increasing dye concentration. This observation is also supported by IEP value (pH = 3) of Congo Red [12].

#### Kinetic Studies

The kinetics of degradation can be mainly studied by pseudo-first order equation. The Langmuir-Hinshelwood (L-H) model was used to describe the kinetics of photocatalytic reactions of aqueous organic pollutants [13]. The (L-H) model relates the degradation rate ( $r$ ) and reactant concentration in water at time  $t$  which is expressed as

$$r = \frac{-dC}{dt} = k_{app} \times C$$

Integrating and using boundary condition  $C = C_0$  at  $t = 0$  and  $C_t$  is dye concentration at time  $t$  we get,

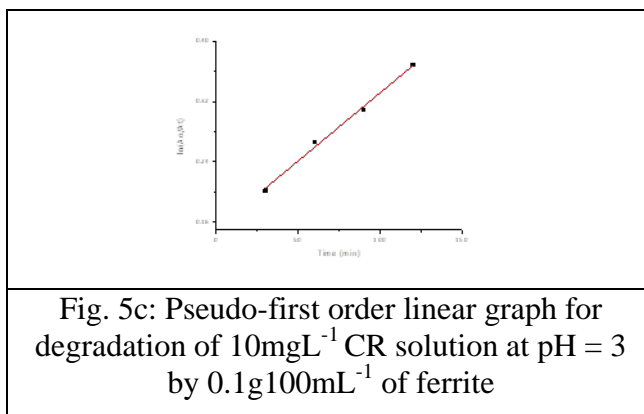
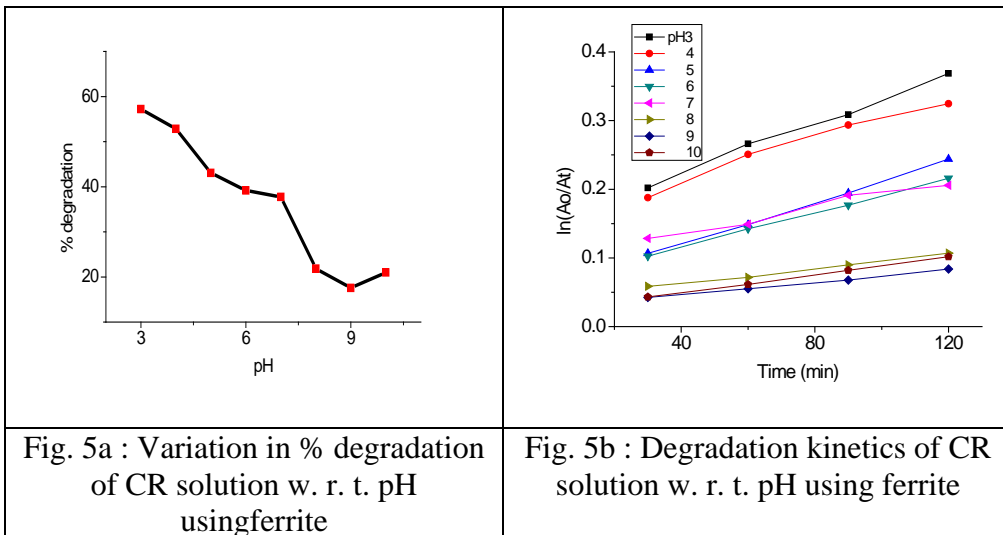
$$\ln \frac{C_0}{C_t} = k_{app} \times t \text{ or } \ln \frac{A_0}{A_t} = k_{app} \times t$$

Where  $k_{app}$  is the apparent rate constant of a pseudo first order reaction,  $A_0$  is initial absorbance and  $A_t$  is absorbance at time  $t$ .

Fig. 5b shows degradation kinetics of CR solution w. r. t. pH using the ferrite. The reaction rate constants ( $K_{app}$ ) for the photo catalyst was determined from the slope of the linearly fitted curves (Fig. 5c for pH = 3) by means of linear regression and the values are given in Table 1. All the plots show a linear relationship with good correlation coefficient ( $R^2 > 0.9$ ), indicating that CR degradation by synthesized ferrites under UV light follows pseudo-first order kinetic model. pH study shows that ferrite is best at pH = 3 with maximum apparent reaction rate constants  $k_{app}$ . Highest  $k_{app}$ ,  $1.81 \times 10^{-3} \text{ min}^{-1}$  with  $R^2$  value 0.99192 was calculated for  $Ni_{0.4}Zn_{0.6}Fe_2O_4$ .

Table 1: Percentage degradation and pseudo first order kinetic parameter of CR dye w. r. t. pH using ferrite

Sr. No.	pH	% Degradation	$K_{app}(\text{min}^{-1})$	$R^2$
1.	3	57.22	$1.81 \times 10^{-3}$	0.99192
2.	4	52.82	$1.51 \times 10^{-3}$	0.96303
3.	5	43.06	$1.53 \times 10^{-3}$	0.99793
4.	6	39.19	$1.25 \times 10^{-3}$	0.99881
5.	7	37.73	$9.14 \times 10^{-4}$	0.94848
6.	8	21.84	$5.43 \times 10^{-4}$	0.99344
7.	9	17.56	$4.55 \times 10^{-4}$	0.99386
8.	10	20.99	$6.56 \times 10^{-4}$	0.99916



### 3.5.2 Effect of photocatalyst loading

The effect of photo catalyst loading was investigated for the synthesized ferrites Ni<sub>0.4</sub>Zn<sub>0.6</sub>Fe<sub>2</sub>O<sub>4</sub> by adding various amounts of catalyst in the range of 0.05-0.3 g into the beaker containing 100 mL of 10 mgL<sup>-1</sup> dye solution at pH = 3, for all experiments. The removal of Congo red at different doses is shown in Fig.6a-b. It was found that with increase in catalyst doses the removal percentage of dye increases. At equilibrium, the percentage of dye removal was found to increase from 26.33% to 82.03% for Ni<sub>0.4</sub>Zn<sub>0.6</sub>Fe<sub>2</sub>O<sub>4</sub> with increase of catalyst doses from 0.05g to 0.3g respectively. The increase in percentage of dye removal with increasing catalyst dosage is due to increase of sorption active sites at the catalyst surface [14].

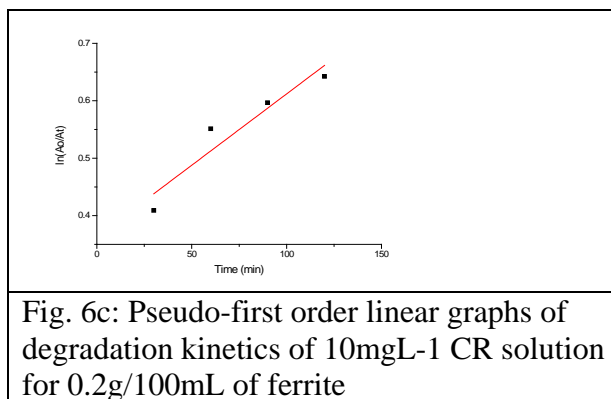
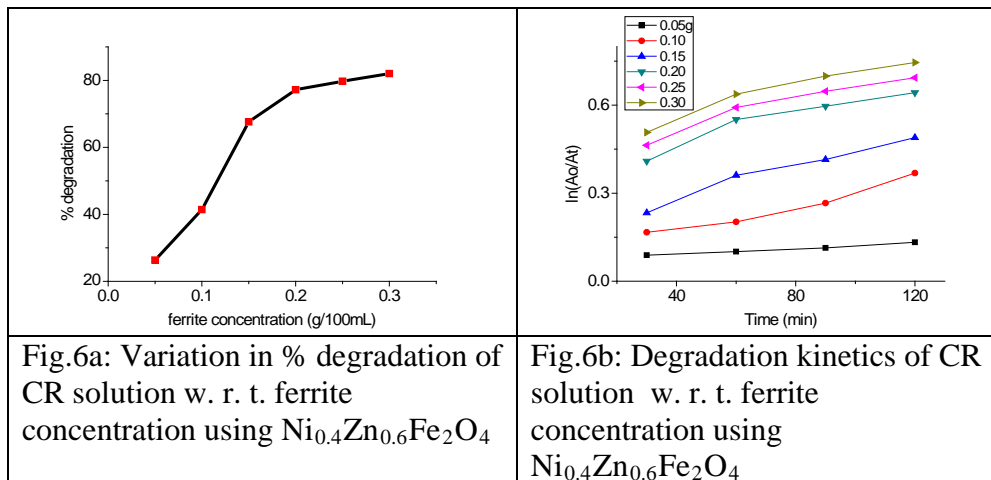
### Kinetic Studies

The degradation pattern suggested that degradation of CR follows pseudo-first order kinetics. The reaction rate constants (K<sub>app</sub>) for different concentrations (0.05g to 0.3g/100mL) of the ferrite was determined from the slope of the fitted curves (Fig.6c for 0.2g/100mL) by means of linear regression and the values are given in Table 2. All the plots show a linear relationship with good correlation coefficient (R<sup>2</sup> > 0.9) indicating that CR degradation by synthesized ferrite under UV light follows pseudo-first order kinetic model. Further, with increased ferrite concentration reaction rate constants k<sub>app</sub> was found to increase.

Table 2: Percentage degradation and pseudo first order kinetic parameter of CR dye w. r. t. ferrite concentration

Sr. No.	Ferrite Conc. (g/100mL)	% Degradation	K <sub>app</sub> (min <sup>-1</sup> )	R <sup>2</sup>
1.	0.05	26.33	4.82 x 10 <sup>-4</sup>	0.98184
2.	0.10	57.22	2.23 x 10 <sup>-3</sup>	0.92784

3.	0.15	67.6	$2.74 \times 10^{-3}$	0.94989
4.	0.20	77.22	$2.48 \times 10^{-3}$	0.8627
5.	0.25	79.75	$2.49 \times 10^{-3}$	0.90286
6.	0.30	82.03	$2.59 \times 10^{-3}$	0.91029



### 3.5.3 Effect of initial dye concentration

Photo degradation of Congo red, as a function of initial dye concentration was studied for 0.2 g of catalyst in 100 mL dye solution at pH = 3 for 2 hrs contact time. The concentration of CR solution was varied from 10mgL<sup>-1</sup> to 50 mgL<sup>-1</sup> maintaining same experimental conditions. The results are shown in Fig. 7a-b. It is clear from the figures that removal percentage of the Congo red dye is high at lower concentration and comparatively decreases with increase in dye concentration. This can be explained as the dye concentration increases, more number of dye molecules get adsorbed on the surface of photo catalyst. Therefore, less number of photons is able to reach catalyst surface generating less amount of hydroxyl free radicals

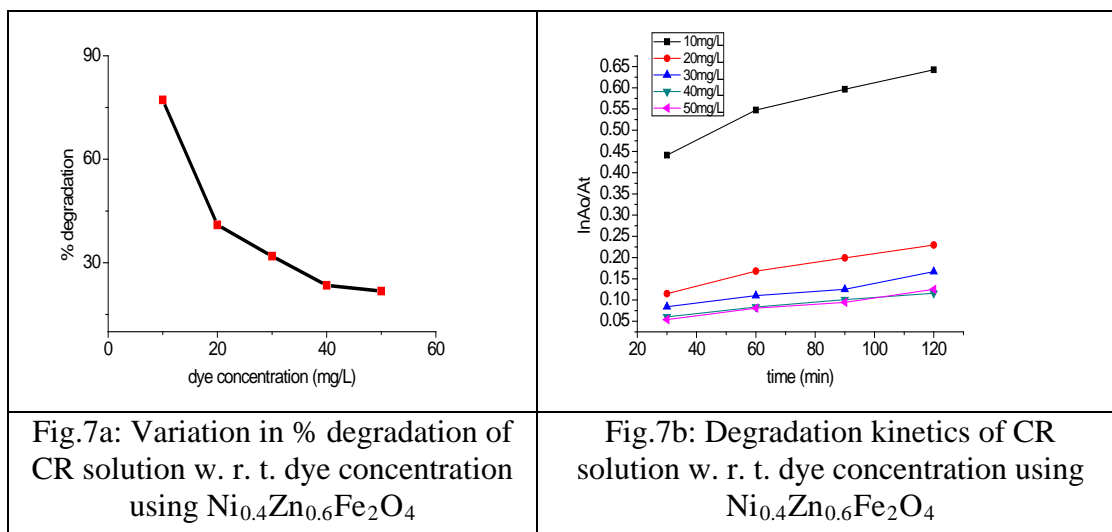
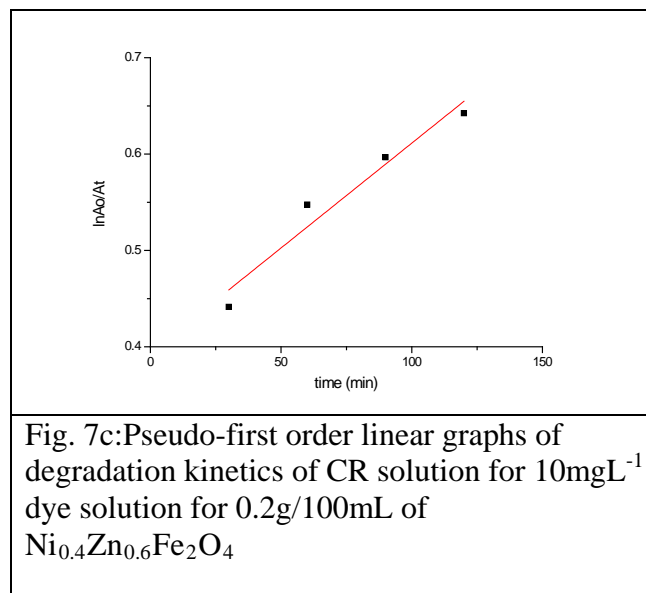
and hence reduction in photo degradation efficiency is observed.

### Kinetic Studies

The reaction rate constants ( $K_{app}$ ) for the ferrite obtained by varying dye concentrations were determined from the slope of the linearly fitted curves (Fig. 7c, for 10mgL<sup>-1</sup> dye) by means of linear regression and the values are given in Table 3. The plots show a linear relationship with good correlation coefficient ( $R^2 > 0.9$ ), indicating that CR degradation by synthesized ferrites under UV light follows pseudo-first order kinetic model. Further, it is observed that with increased dye concentration, reaction rate constant  $k_{app}$  is decreased.

Table 3: Percentage degradation and pseudo first order kinetic parameters w. r. t. CR dye concentration for ferrite

Sr. No.	Dye Conc. (mg/L)	% Degradation	$K_{app}(\text{min}^{-1})$	$R^2$
1.	10	77.22	$2.17 \times 10^{-3}$	0.92936
2.	20	40.96	$1.25 \times 10^{-3}$	0.96857
3.	30	31.92	$8.78 \times 10^{-4}$	0.94418
4.	40	23.45	$6.16 \times 10^{-4}$	0.98472
5.	50	21.78	$7.60 \times 10^{-4}$	0.97161

Fig.7a: Variation in % degradation of CR solution w. r. t. dye concentration using  $\text{Ni}_{0.4}\text{Zn}_{0.6}\text{Fe}_2\text{O}_4$ Fig.7b: Degradation kinetics of CR solution w. r. t. dye concentration using  $\text{Ni}_{0.4}\text{Zn}_{0.6}\text{Fe}_2\text{O}_4$ Fig. 7c: Pseudo-first order linear graphs of degradation kinetics of CR solution for  $10\text{mgL}^{-1}$  dye solution for 0.2g/100mL of  $\text{Ni}_{0.4}\text{Zn}_{0.6}\text{Fe}_2\text{O}_4$ 

### Conclusion

The photo catalytic degradation of Congo red was carried out successfully using zinc substituted nickel ferrite  $\text{Ni}_{0.6}\text{Zn}_{0.4}\text{Fe}_2\text{O}_4$  synthesized by sol gel auto combustion method. The ferrite was characterized by XRD, FTIR, SEM-EDX and TEM spectroscopic techniques. Maximum photo catalytic activity of spinel

ferrite was observed for 0.3g ferrite for 100 mL dye solution at pH = 3 for 2 hrs contact time.

### References

1. Akpan, U. G., Hameed, B. H. (2009). Parameters affecting the photocatalytic degradation of dyes. *J. Hazard. Mater.*, 170(2-3), 520-529.

2. Pearce, C. I., Lloyd, J. R., Guthrie, J. T. (2003). The removal of colour from textile wastewater using whole bacterial cells: a review. *Dyes and Pigments*, 58(3), 179-196.
3. Robinson, T., McMullan, G., Marchant, R., Nigam, P. (2001). Remediation of dyes in textile effluent: a critical review on current treatment technologies with a proposed alternative. *Bioresource Technology*, 77(3), 247-255.
4. Kulkarni, M., Thakur, P. (2014). Synthesis of silver doped TiO<sub>2</sub> nanoparticles for the improved photocatalytic degradation of methyl orange. *Int. J. Eng. Res. Gen. Sci.*, 2, 245-254.
5. Yogendra, K., Naik, S., Mahadevan, K.M., Madhusudhana, N. (2011). A comparative study of photocatalytic activities of two different synthesized ZnO composites against Coralene Red F3BS dye in presence of natural solar light. *Int. J. Environ. Sci. Res.*, 1(1), 11-15.
6. Bhukal, S., Namgyal, T., Mor, S., Bansal, S., Singhal, S. (2012). Structural, electrical, optical and magnetic properties of chromium substituted Co-Zn nanoferrites Co<sub>0.6</sub>Zn<sub>0.4</sub>Cr<sub>x</sub>Fe<sub>2-x</sub>O<sub>4</sub> (0 ≤ x ≤ 1.0) prepared via sol-gel auto-combustion method. *J. Mol. Struct.*, 1012, 162-167.
7. Lwin, N., Othman, R., Noor, A. F. M., Sreekantan, S., Yong, T. C., Singh, R., Tin, C. C. (2015). Influence of pH on the physical and electromagnetic properties of Mg-Mn ferrite synthesized by a solution combustion method. *Materials Characterization*, 110, 109-115.
8. Raming, T. P., Winnubst, A. J. A., Van Kats, C. M., Philipse, P. (2002). The Synthesis and Magnetic Properties of Nanosized Hematite (α-Fe<sub>2</sub>O<sub>3</sub>) Particles. *Journal of Colloid and Interface Science*, 249, 346-350.
9. Jothiramalingam, R., Wang, M. K. (2007). Synthesis, characterization and photocatalytic activity of porous manganese oxide doped titania for toluene decomposition. *J. Hazardous Mat*, 147, 562-569.
10. Singh, B. P., Menchavez, R., Takai, C., Fuji, M., Takahashi, M. (2005). Stability of Dispersions of Colloidal Alumina Particles in Aqueous Suspensions. *J. Colloid. Inter. Sci.*, 291, 181-186.
11. Bonancea, C. E., do Nascimento, G. M., de Souza, M. L., Temperini, M. L. A., Corio, P. (2006). *Appl. Catal. B - Environ.*, 69, 34-42.
12. Ahmad, R., Kumar, R. (2010). Adsorptive removal of Congo red dye from aqueous solution using bael shell carbon *Appl. Surf. Sci.*, 257, 1628-1633.
13. Tanveer, M., Cao, C., Aslam, I., Ali, Z., Idrees, F., Tahir, M., Khan, W. S., Butt, F. K., Mahmood, A. (2014). Effect of the morphology of CuS upon the photocatalytic degradation of organic dyes *RSC Adv.*, 4, 63447-63456.
14. Royer, B., Cardoso, N. F., Lima, E. C., Vaghetti, J. C. P., Simon, N. M., Calvete, T., Veses, R. C. (2009). Applications of Brazilian-pine fruit shell in natural and carbonized forms as adsorbents to removal of methylene blue from aqueous solutions – kinetic and equilibrium study. *J. Hazard. Mater.*, 164, 1213-1222.